AD-A134 026 THE DEVELOPMENT OF A NUMERICAL SOLUTION TO THE TRANSPORT EQUATION REPORT 3 TEST RESULTS(U) COASTAL ENGINEERING RESEARCH CENTER VICKSBURG MS R A SCHMALZ 1/1

UNCLASSIFIED SEP 83 CERC-83-2/3 F/G 8/8 NL

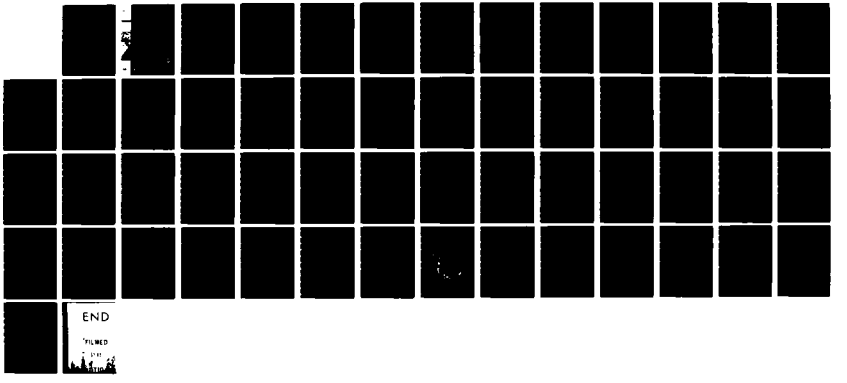

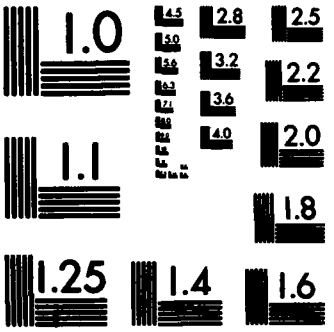

MICROCOPY RESOLUTION TEST CHART
NATIONAL BUREAU OF STANDARDS-1963-A

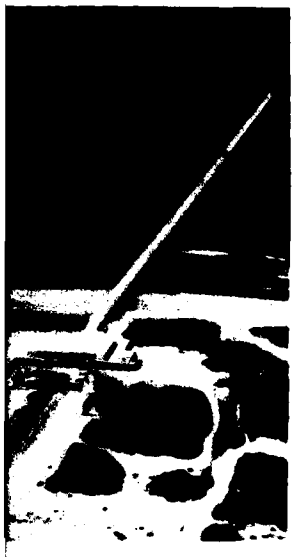

MISCELLANEOUS PAPER CERC-83-2

THE DEVELOPMENT OF A NUMERICAL SOLUTION TO THE TRANSPORT EQUATION

Report 3

TEST RESULTS

by

R. A. Schmalz, Jr.

Coastal Engineering Research Center
U. S. Army Engineer Waterways Experiment Station
P. O. Box 631, Vicksburg, Miss. 39180

September 1983
Report 3 of a Series

Prepared for U. S. Army Engineer District, Mobile
Mobile, Ala. 36628

Destroy this report when no longer needed. Do not return it to the originator.

The findings in this report are not to be construed as an official Department of the Army position unless so designated by other authorized documents.

The contents of this report are not to be used for advertising, publication, or promotional purposes. Citation of trade names does not constitute an official endorsement or approval of the use of such commercial products.

Unclassified

SECURITY CLASSIFICATION OF THIS PAGE *(When Data Entered)*

REPORT DOCUMENTATION PAGE	READ INSTRUCTIONS BEFORE COMPLETING FORM
1. REPORT NUMBER Miscellaneous Paper CERC-83-2	2. GOVT ACCESSION NO. A134026
	3. RECIPIENT'S CATALOG NUMBER
4. TITLE *(and Subtitle)* DEVELOPMENT OF A NUMERICAL SOLUTION TO THE THE TRANSPORT EQUATION; Report 3: TEST RESULTS	5. TYPE OF REPORT & PERIOD COVERED Report 3 of a series
	6. PERFORMING ORG. REPORT NUMBER
7. AUTHOR(s) Richard A. Schmalz, Jr.	8. CONTRACT OR GRANT NUMBER(s)
9. PERFORMING ORGANIZATION NAME AND ADDRESS U. S. Army Engineer Waterways Experiment Station Coastal Engineering Research Center P. O. Box 631, Vicksburg, Miss. 39180	10. PROGRAM ELEMENT, PROJECT, TASK AREA & WORK UNIT NUMBERS
11. CONTROLLING OFFICE NAME AND ADDRESS U. S. Army Engineer District, Mobile P. O. Box 2208 Mobile, Ala. 36628	12. REPORT DATE September 1983
	13. NUMBER OF PAGES 51
14. MONITORING AGENCY NAME & ADDRESS(*if different from Controlling Office*)	15. SECURITY CLASS. *(of this report)* Unclassified
	15a. DECLASSIFICATION/DOWNGRADING SCHEDULE

16. DISTRIBUTION STATEMENT *(of this Report)*

Approved for public release; distribution unlimited.

17. DISTRIBUTION STATEMENT *(of the abstract entered in Block 20, if different from Report)*

18. SUPPLEMENTARY NOTES

Available from National Technical Information Service, 5285 Port Royal Road, Springfield, Va. 22161.

19. KEY WORDS *(Continue on reverse side if necessary and identify by block number)*

Finite differences	Salinity
Mississippi Sound	Transport
Numerical modeling	Variable grid

20. ABSTRACT *(Continue on reverse side if necessary and identify by block number)*

This report, Report 3 in a three-report series, presents the results of numerical experiments using the following schemes developed in the first two reports of the series: (1) Forward Time Upwind Space (FTUS), (2) Forward Time Centered Space (FTCS), (3) Spread Time Derivative Upwind Space (STUS), (4) Spread Time Derivative Centered Space (STCS), and (5) Flux Corrected Transport (FCT). Experimental results on a 7 by 8 uniform grid are directly

(Continued)

DD FORM 1 JAN 73 1473 EDITION OF 1 NOV 65 IS OBSOLETE

Unclassified

SECURITY CLASSIFICATION OF THIS PAGE *(When Data Entered)*

20. ABSTRACT (Continued).

compared with analytical solutions for several sharp front problems. A 60 by 60 square grid was employed subsequently to test boundary condition effects. Based upon the uniform grid test results, the FCT scheme was incorporated within the U. S. Army Engineer Waterways Experiment Station Implicit Flooding Model (WIFM) and employed to simulate a sharp front problem on a variably spaced 6785-computational-cell global grid representing Mississippi Sound and adjacent areas.

PREFACE

The numerical implementation and testing of approximation procedures to the transport equation are reported herein. The numerical procedures have been incorporated into a numerical model to be used for evaluating effects of proposed dredged material disposal practices in the Mississippi Sound and adjacent areas.

Project administration and funding were provided by the U. S. Army Engineer District, Mobile. Funding for publication was provided by the Coastal Engineering Research Center (CERC).

Numerical implementation and testing were conducted by the U. S. Army Engineer Waterways Experiment Station (WES) in the Hydraulics Laboratory (HL) under the general supervision of Messrs. H. B. Simmons and F. A. Herrmann, Jr., Chief and Assistant Chief, respectively, HL, and in CERC under the general supervision of Drs. R. W. Whalin and L. E. Link, Chief and Assistant Chief, respectively, CERC, and Mr. C. E. Chatham, Chief, Wave Dynamics Division (WDD). This report was prepared by Dr. R. A. Schmalz, Jr., WDD.

Commanders and Directors of WES during data acquisition and analysis and the preparation and publication of this report were COL Nelson P. Conover, CE, and COL Tilford C. Creel, CE. Technical Director was Mr. F. R. Brown.

TABLE OF CONTENTS

LIST OF FIGURES

LIST OF TABLES

CONVERSION FACTORS, INCH-POUND TO METRIC (SI)

UNITS OF MEASUREMENT

Inch-pound units of measurement used in this report can be converted to metric (SI) units as follows:

Multiply	By	To Obtain
cubic feet	0.02831685	cubic meters
feet	0.3048	meters
feet per second (fps)	0.3048	meters per second
parts per thousand (ppt)-cubic feet	0.02831685	grams per liter-cubic meters
square feet	0.09290304	square meters
square feet per second	0.09290304	square meters per second

DEVELOPMENT OF A NUMERICAL SOLUTION TO THE TRANSPORT EQUATION

Report 3: TEST RESULTS

PART I: INTRODUCTION

This report constitutes the third report in a three-report series and presents the development of a test program and the numerical experimentation of several alternate finite difference solution techniques for the constituent transport equation. The following schemes as previously developed [1,2] were considered initially on uniformly spaced grids.

1. Forward Time Upwind Space (FTUS)
2. Forward Time Centered Space (FTCS)
3. Spread Time Derivative Upwind Space (STUS)
4. Spread Time Derivative Centered Space (STCS)
5. Flux-Corrected Transport (FCT)

A 7 × 8 uniform grid was initially employed to verify the coding and to evaluate the effectiveness of the alternate techniques. Experimental results are directly compared with known analytical solutions. Analytical solution techniques are initially presented followed by the test results. A 60 × 60 uniform grid was subsequently employed to test boundary condition effects and spatial resolution accuracy relations.

Based upon the uniform grid test results, the FCT scheme was incorporated into the U. S. Army Engineer Waterways Experiment Station Implicit Flooding Model (WIFM). The FCT scheme was tested for a sharp front problem over the variable spaced global grid employing 6785 computational cells representing Mississippi Sound.

PART II: ANALYTICAL SOLUTION METHODS

The advection, diffusion, and the combined problem are considered here for the constant coefficient case in turn.

1. Advection Problem

Consider the following problems

$$\frac{\partial c}{\partial t} = -u \frac{\partial c}{\partial x} - v \frac{\partial c}{\partial y}$$

$$c(x,y,o) = \psi(x,y) \tag{1.1}$$

where

- $c \equiv$ constituent concentration
- $u \equiv$ velocity component in the x coordinate direction
- $v \equiv$ velocity component in the y coordinate direction
- $x,y \equiv$ Cartesian coordinates
- $t \equiv$ time

Assume u,v are constant. Since $\frac{Dc}{Dt} = \frac{\partial c}{\partial t} + u \frac{\partial c}{\partial x} + v \frac{\partial c}{\partial y}$, (1.1) may be written

$$\frac{Dc}{Dt} = 0 \tag{1.2}$$

From this relation, we observe that the property of the fluid is unchanged with respect to a coordinate system attached to the fluid particles. We thus expect the following solution, $c(x,y,t) = \psi(x - ut, y - vt)$. Since

$$\frac{\partial c}{\partial t} = \frac{\partial[\psi(x - ut, y - vt)]}{\partial x}(-u) + \frac{\partial[\psi(x - ut, y - vt)]}{\partial y}(-v) \tag{1.3}$$

$$\frac{\partial c}{\partial x} = \frac{\partial[\psi(x - ut, y - vt)]}{\partial x} \qquad \frac{\partial c}{\partial y} = \frac{\partial[\psi(x - ut, y - vt)]}{\partial y}$$

our suppositions are indeed substantiated. If we consider

$$\psi(x,y) = \begin{Bmatrix} c_o & x,y \in (-R/2,R/2) \\ o & x,y \notin (-R/2,R/2) \end{Bmatrix}$$

as our initial distribution, then

$$c(x,y,t) = \left\{ \begin{array}{ll} c_o & \begin{Bmatrix} x \in (-R/2 + ut, R/2 + ut) \\ y \in (-R/2 + vt, R/2 + vt) \end{Bmatrix} \\ o & \begin{Bmatrix} x \notin (-R/2 + ut, R/2 + ut) \\ y \notin (-R/2 + vt, R/2 + vt) \end{Bmatrix} \end{array} \right\} = \psi(x - ut, y - vt) \qquad (1.4)$$

The distribution is translated in space with no distortion.

2. Diffusion Problem

Consider the following problem, using the same notation as in (1.1):

$$\frac{\partial c}{\partial t} = a^2\left(\frac{\partial^2 c}{\partial x^2} + \frac{\partial^2 c}{\partial y^2}\right) \qquad (2.1)$$

$$c(x,y,o) = \psi(x,y)$$

We follow an approach developed by Polzhiy [3] for the one-dimensional equation. Assume a solution of the following form:

$$I(x,y,t) = c(x,y,t)$$

$$= \left(\int_{-\infty}^{\infty} e^{-\alpha^2 a^2 t} \cos \alpha x \, d\alpha\right)\left(\int_{-\infty}^{\infty} e^{-\alpha^2 a^2 t} \cos \alpha y \, d\alpha\right) \qquad (2.2)$$

Since

$$\frac{\partial I}{\partial t} = -2\alpha^2 a^2 I \quad \text{and} \quad \frac{\partial^2 I}{\partial x^2} = \frac{\partial^2 I}{\partial y^2} = -\alpha^2 I$$

(2.2) satisfies (2.1) above. Next we compute

$$\frac{\partial I}{\partial x} = -\alpha \int_{-\infty}^{\infty} e^{-\alpha^2 a^2 t} \sin \alpha x \, d\alpha \left(\int_{-\infty}^{\infty} e^{-\alpha^2 a^2 t} \cos \alpha y \, d\alpha \right) \tag{2.3a}$$

$$\frac{\partial I}{\partial y} = -\alpha \int_{-\infty}^{\infty} e^{-\alpha^2 a^2 t} \sin \alpha y \, d\alpha \left(\int_{-\infty}^{\infty} e^{-\alpha^2 a^2 t} \cos \alpha x \, d\alpha \right) \tag{2.3b}$$

We next integrate the first factor in (2.2) by parts; i.e., $\int udv = uv - \int vdu$. Letting $u = e^{-\alpha^2 a^2 t}$ and $dv = \cos \alpha x \, d\alpha$, we obtain

$$\int_{-\infty}^{\infty} e^{-\alpha^2 a^2 t} \cos \alpha x \, d\alpha = x^{-1} \sin \alpha x e^{-\alpha^2 a^2 t} \Big|_{-\infty}^{\infty} + 2a^2 t x^{-1} \int_{-\infty}^{\infty} \alpha e^{-\alpha^2 a^2 t} \sin \alpha x \, d\alpha \tag{2.4}$$

Noting the first term on the right hand side of (2.4) is zero we obtain the following alternate form for (2.2) using (2.3a):

$$I(x,y,t) = -2a^2 t x^{-1} \left(-\alpha \int_{-\infty}^{\infty} e^{-\alpha^2 a^2 t} \sin \alpha x \, d\alpha \right) \times \left(\int_{-\infty}^{\infty} e^{-\alpha^2 a^2 t} \cos \alpha y \, d\alpha \right) = -2a^2 t x^{-1} \frac{\partial I}{\partial x} \tag{2.5}$$

By integrating the second factor in (2.2) by parts and using (2.3b) we also obtain a similar relationship with x and y interchanged.

$$I(x,y,t) = -2a^2 t y^{-1}\left(-\alpha \int_{-\infty}^{\infty} e^{-\alpha^2 a^2 t} \sin \alpha y \, d\alpha\right) \tag{2.6}$$

$$\times \left(\int_{-\infty}^{\infty} e^{-\alpha^2 a^2 t} \cos \alpha x \, d\alpha\right) = -2a^2 t y^{-1} \frac{\partial I}{\partial y}$$

Equations (2.5) and (2.6) suggest the following relation for $I(x,y,t)$:

$$\frac{\partial I}{\partial x} = \frac{-x}{2a^2 t} I \qquad \frac{\partial I}{\partial y} = \frac{-y}{2a^2 t} I \rightarrow I(x,y,t) = Ce^{-(x^2+y^2)/(4a^2 t)} \tag{2.7}$$

Consider

$$I(o,o,t) = \left(\int_{-\infty}^{\infty} e^{-\alpha^2 a^2 t} \, d\alpha\right)\left(\int_{-\infty}^{\infty} e^{-\alpha^2 a^2 t} \, d\alpha\right) = C \tag{2.8}$$

It may be shown that each factor is equal to $\frac{\sqrt{\pi}}{a\sqrt{t}}$.

Thus $C = \frac{\pi}{a^2 t}$ and we finally obtain:

$$I(x,y,t) = \frac{\pi}{a^2 t} e^{-(x^2+y^2)/(4a^2 t)} \tag{2.9}$$

The following δ function is also a solution

$$\delta(P,P',t-t') = \frac{1}{4\pi^2} I(x - x', y - y', t - t') = \frac{1}{4a^2 \pi (t-t')} e^{-r^2/[4a^2(t-t')]}$$

where

$$r = \sqrt{(x - x')^2 + (y - y')^2} \, , \quad t > t'$$

The above set of functions with parameter $\alpha = t - t'$, have the three special properties.

$$\int_{-\infty}^{\infty}\int_{-\infty}^{\infty} \delta(P,P',t-t')\,dx\,dy = \int_{-\infty}^{\infty} \frac{1}{2a\sqrt{\pi(t-t')}}\, e^{-(x-x')^2/[4a^2(t-t')]}\, dx \int_{-\infty}^{\infty} \frac{1}{2a\sqrt{\pi(t-t')}}\, e^{-(y-y')^2/[4a^2(t-t')]}\, dy = 1 \tag{2.10a}$$

$$\iint_{-\infty}^{\infty} |\delta(P,P',t-t')|\,dx\,dy = 1. \tag{2.10b}$$

$$\lim_{\substack{t\to t'\\ +}} \int_{-\infty}^{\infty}\int_{-\infty}^{\infty}{}' |\delta(P,P',t-t')|\,dx\,dy = 0 \tag{2.10c}$$

The prime on the integral in (2.10c) denotes integration over the entire x-y space except for an arbitrarily small neighborhood about P'. Thus, after concepts of Polzhiy [3], the limit element of the sequence of functions generated when $\alpha \to 0$, in the sense of weak convergence, is a δ-function with respect to M^*, the set of all continuous bounded functions of x and y. Thus noting $\delta(P,P',t-t') = \delta(P',P,t-t')$:

$$\lim_{\substack{t\to t'\\ +}} \left\{\int_{-\infty}^{\infty} f(x') \frac{1}{2a\sqrt{\pi(t-t')}}\, e^{-(x-x')^2/[4a^2(t-t')]}\, dx'\right\} \times \left\{\int_{-\infty}^{\infty} g(y') \frac{1}{2a\sqrt{\pi(t-t')}}\, e^{-(y-y')^2/[4a^2(t-t')]}\, dy'\right\} = f(x)g(y) \tag{2.11}$$

where

$$\psi(x,y) = f(x)g(y)$$

We therefore obtain a solution of the form, where $t' = 0$

$$c(x,y,t) = \left[\int_{-\infty}^{\infty} f(x') \frac{1}{2a\sqrt{\pi t}} e^{-(x'-x)^2/(4a^2t)}\, dx'\right] \times \left[\int_{-\infty}^{\infty} g(y') \frac{1}{2a\sqrt{\pi t}} e^{-(y'-y)^2/(4a^2t)}\, dy'\right] \tag{2.12}$$

From (2.11) we note (2.12) satisfies the initial condition.

Consider the following problem

$$f(x)g(y) = \psi(x,y) = \begin{cases} c_o & x,y \in (-R/2,R/2) \\ o & x,y \notin (-R/2,R/2) \end{cases} \tag{2.13}$$

and

$$\frac{\partial c}{\partial t} = K\left(\frac{\partial^2 c}{\partial x^2} + \frac{\partial^2 c}{\partial y^2}\right)$$

Evaluating (2.12) we obtain

$$c(x,y,t) = \left[\int_{-R/2}^{R/2} \frac{\sqrt{c_o}}{2\sqrt{K\pi t}} e^{-(x'-x)^2/(4Kt)}\, dx'\right] \times \left[\int_{-R/2}^{R/2} \frac{\sqrt{c_o}}{2\sqrt{K\pi t}} e^{-(y'-y)^2/(4Kt)}\, dy'\right] \tag{2.14}$$

Consider (2.14) in the following manner:

$$r = (x - x')/2\sqrt{Kt} \qquad dr = -dx'/2\sqrt{Kt}$$

$$s = (y - y')/2\sqrt{Kt} \qquad ds = -dy'/2\sqrt{Kt}$$

then

$$c(x,y,t) = \left[\frac{\sqrt{c_o}}{\sqrt{\pi}} \int_{(x-R/2)/2\sqrt{Kt}}^{(x+R/2)/2\sqrt{Kt}} e^{-r^2}\, dr\right]\left[\frac{\sqrt{c_o}}{\sqrt{\pi}} \int_{(y-R/2)/2\sqrt{Kt}}^{(y+R/2)/2\sqrt{Kt}} e^{-s^2}\, ds\right] \tag{2.15}$$

Noting

$$\operatorname{erf}(x) = \frac{2}{\sqrt{\pi}}\int_0^x e^{-r^2}\, dr = \frac{2}{\sqrt{\pi}} \int_{-x}^{o} e^{-r^2}\, dr \quad ,$$

the above result may be further simplified to the following form:

$$c(x,y,t) = \frac{c_o}{4}\left\{\operatorname{erf}[(x + R/2)/2\sqrt{Kt}] + \operatorname{erf}[(R/2 - x)/2\sqrt{Kt}]\right\} \times \left\{\operatorname{erf}[(y + R/2)/2\sqrt{Kt}] + \operatorname{erf}[(R/2 - y)/2\sqrt{Kt}]\right\} \tag{2.16}$$

3. Advection and Diffusion Problem

Consider the following problem

$$\frac{Dc}{Dt} = \frac{\partial c}{\partial t} + u\frac{\partial c}{\partial x} + v\frac{\partial c}{\partial y} = K\left(\frac{\partial^2 c}{\partial x^2} + \frac{\partial^2 c}{\partial y^2}\right) \tag{3.1}$$

$$c(x,y,o) = \psi(x,y) = f(x)g(y)$$

where u and v are constant. Define

$$G(x,y,t) = \left\{\int_{-\infty}^{\infty} f(x')\left[\frac{1}{2\sqrt{K\pi t}} e^{-(x-x')^2/(4Kt)}\right]dx'\right\} \times \left\{\int_{-\infty}^{\infty} g(y')\left[\frac{1}{2\sqrt{K\pi t}} e^{-(y-y')^2/(4Kt)}\right]dy'\right\} \tag{3.2}$$

We assume a solution $c(x,y,t) = G(x - ut, y - vt, t)$. It may be shown by computing $\partial c/\partial t$, $\partial c/\partial x$, $\partial c/\partial y$, $\partial^2 c/\partial x^2$, $\partial^2 c/\partial y^2$, that the solution assumed satisfies (3.1). Furthermore, from previous work (3.2) satisfies the initial condition and are assumed solution is the solution.

We consider $\psi(x,y)$ to be as given previously, namely, our familiar block distribution problem. Employing previous results, the solution assumes the following form.

$$c(x,y,t) = \frac{c_o}{4}\left\{\text{erf}[(x - ut + R/2)/2\sqrt{Kt}] + \text{erf}[(ut - x + R/2)/2\sqrt{Kt}]\right\}$$

$$\times\left\{\text{erf}[(y - vt + R/2)/2\sqrt{Kt}] + \text{erf}[(vt - y + R/2)/2\sqrt{Kt}]\right\} \quad (3.3)$$

PART III: SMALL GRID (7 × 8) TEST RESULTS

Several tests were performed employing this grid both on the Kirtland Air Force Base (CRAY-1) and the Boeing Computer Service (CRAY-1) computers. The problems considered and numerical results are presented in turn. In characterizing the test cases, the following dimensionless parameters are employed:

$$\mathcal{U} = \frac{u\tau}{\Delta x} \qquad \mathcal{D}_x = \frac{K_x \tau}{\Delta x^2} \qquad Pe_x = \frac{\mathcal{U}}{\mathcal{D}_x}$$

$$\mathcal{V} = \frac{v\tau}{\Delta x} \qquad \mathcal{D}_y = \frac{K_x \tau}{\Delta y^2} \qquad Pe_y = \frac{\mathcal{V}}{\mathcal{D}_y}$$

where

τ = Simulation time step length (seconds)

Δx = x space step (feet*)

Δy = y space step (feet)

K_x = Dispersion coefficient in the x direction

K_y = Dispersion coefficient in the y direction

$\mathcal{U}$ = Particle Courant number in the x direction

$\mathcal{V}$ = Particle Courant number in the y direction

$\mathcal{D}_x$ = Diffusion number in the x direction

$\mathcal{D}_y$ = Diffusion number in the y direction

Pe_x = Peclet number in the x direction

Pe_y = Peclet number in the y direction

---

* A table for converting the inch-pound units of measurement found in this report to metric (SI) units can be found on page 5.

1. Block Translation Problem

The pure translation of a square block of concentration 1 ppt initially occupying grid cell (3,6) as shown in Figure 1 was considered. Particle Courant numbers of 0.2 in both coordinate directions were maintained for ten time steps of 100 seconds duration.

The problem represented an extremely severe test for the solution schemes considered, since a discontinuity was introduced over only 1 grid cell in both directions. The analytical solution consists of a unit concentration in cell (5,4) after 100 seconds.

Results for the FTUS scheme are presented in Figure 2. The scheme exhibits considerable frontal smearing but is nonoscillatory. The FTCS scheme results in Figure 3 contain 122 versus 74 ppt $\times 10^{-3}$ of the FTUS scheme in cell (5,4) at the end of the simulation. However, the FTCS develops severe oscillations behind the front. Results for the STUS scheme are given in Figure 4 and are similar to those of the FTUS scheme. Results for the STCS scheme of Figure 5 are similar to the FTCS scheme results. The FCT scheme results in Figure 6 are nonoscillatory and also exhibit a certain amount of frontal smearing.

All schemes considered exhibited numerical dispersion and subsequent loss of mass through the grid boundary. The schemes were ranked in Table I on their ability to maintain material on the grid. The FCT scheme is the most accurate scheme based upon this criterion. In Table II the schemes are ranked according to their ability to place the most material in the correct cell (5,4). The FCT scheme ranked first in maintaining material on the grid and was also the top ranked nonoscillatory scheme in terms of mass placement.

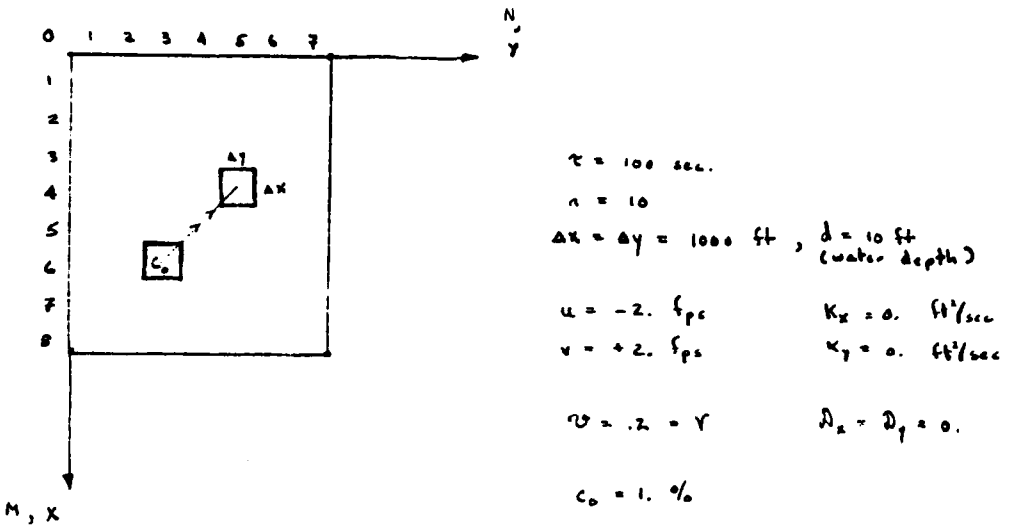

Figure 1. Pure translation of a block (small grid case)

Time Step No. 10 Time = 1000.00 Concentration Field ($\times 10^3$)

	N						
M	1	2	3	4	5	6	7
1	0.	0.	0.	0.	0.	0.	0.
2	0.	0.	12.	24.	24.	16.	0.
3	0.	0.	24.	49.	49.	32.	0.
4	0.	0.	37.	74.	74.	49.	0.
5	0.	0.	37.	74.	74.	49.	0.
6	0.	0.	18.	37.	37.	24.	0.
7	0.	0.	0.	0.	0.	0.	0.
8	0.	0.	0.	0.	0.	0.	0.

(FTUS) Mass Grid Total 0.812556×10^7 ppt-ft^3

Figure 2. Pure translation of a block (small grid case) FTUS

Time Step No. 10 Time = 1000.00 Concentration Field ($\times 10^3$)

	N						
M	1	2	3	4	5	6	7
1	0.	0.	0.	0.	0.	0.	0.
2	0.	-25.	7.	20.	12.	5.	0.
3	0.	-90.	25.	73.	45.	17.	0.
4	0.	-247.	67.	200.	122.	47.	0.
5	0.	-402.	110.	325.	199.	77.	0.
6	0.	-136.	37.	110.	67.	26.	0.
7	0.	498.	-136.	-402.	-246.	-96.	0.
8	0.	0.	0.	0.	0.	0.	0.

(FTCS) Mass Grid Total 0.308442×10^7 ppt-ft^3

Figure 3. Pure translation of a block (small grid case) FTCS

Time Step No. 10 Time = 1000.00 Concentration Field ($\times 10^3$)

	N						
M	1	2	3	4	5	6	7
1	0.	0.	0.	0.	0.	0.	0.
2	0.	4.	13.	25.	30.	25.	0.
3	0.	7.	25.	48.	58.	50.	0.
4	0.	9.	31.	60.	72.	62.	0.
5	0.	7.	25.	49.	59.	50.	0.
6	0.	4.	13.	26.	31.	27.	0.
7	0.	1.	4.	8.	10.	8.	0.
8	0.	0.	0.	0.	0.	0.	0.

(STUS) Mass Grid Total 0.837683×10^7 ppt-ft^3

Figure 4. Pure translation of a block (small grid case) STUS

Time Step No. 10 Time = 1000.00 Concentration Field ($\times 10^3$)

	N						
M	1	2	3	4	5	6	7
1	0.	0.	0.	0.	0.	0.	0.
2	0.	5.	7.	-10.	-13.	-3.	0.
3	0.	-39.	-56.	74.	57.	21.	0.
4	0.	-161.	-228.	303.	398.	88.	0.
5	0.	-116.	-164.	219.	287.	63.	0.
6	0.	147.	208.	-277.	-363.	-80.	0.
7	0.	154.	218.	-291.	-382.	-84.	0.
8	0.	0.	0.	0.	0.	0.	0.

(STCS) Mass Grid Total $0.240733E-01 \times 10^7$ ppt-ft^3

Figure 5. Pure translation of a block (small grid case) STCS

Time Step No. 10 Time = 1000.00 Concentration Field ($\times 10^3$)

	N						
M	1	2	3	4	5	6	7
1	0.	0.	0.	0.	0.	0.	0.
2	0.	0.	3.	12.	8.	2.	0.
3	0.	0.	14.	52.	36.	10.	0.
4	0.	0.	35.	127.	91.	28.	0.
5	0.	0.	59.	161.	129.	41.	0.
6	0.	0.	8.	59.	36.	10.	0.
7	0.	0.	0.	0.	0.	0.	0.
8	0.	0.	0.	0.	0.	0.	0.

(FCT) Mass Grid Total 0.920873×10^7 ppt-ft^3

Figure 6. Pure translation of a block (small grid case) FCT

Table I. Block Translation Scheme Rankings (Mass Retention)

Scheme	Material Remaining on Grid (ppt × 10^7 ft^3)
1. FCT	0.920873
2. STUS	0.837683
3. FTUS	0.812556
4. FTCS	0.308442
5. STCS	0.024073

Table II. Block Translation Scheme Rankings (Mass Placement)

Scheme	Material in Cell (5,4) (ppt)
1. STCS*	0.398
2. FTCS*	0.122
3. FCT	0.091
4. FTUS	0.074
5. STUS	0.072

* Oscillatory solution.

2. Stationary Block Problem

The stationary block problem specified initially a 1-ppt (%) concentration in grid cell (3,6) as shown in Figure 7. No diffusion and no advection were considered and the schemes were tested on their ability to maintain the unit concentration in the grid cell for 10 time steps of 100 seconds each.

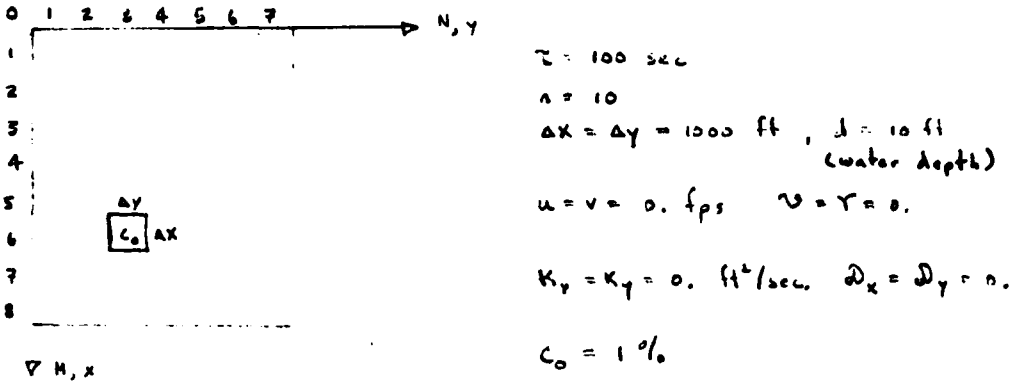

Figure 7. Stationary block problem (small grid case)

The STUS and STCS schemes are equivalent for this problem. The results of the STCS scheme are shown in Figure 8. Note the tendency toward oscillation. The FTUS, FTCS, and FCT schemes are equivalent for this problem. The results of the FCT scheme are shown in Figure 9 and show no tendency toward oscillation.

3. Block Diffusion Problem

The straight diffusion of a square block of 1-ppt concentration initially occupying grid cell (3,6) as shown in Figure 10 was considered. Diffusion numbers of 0.0001 in both coordinate directions were maintained for ten time-steps of 100 seconds each. Analytical solution results indicated a negligible amount of diffusion of material from grid cell (3,6).

The results of STCS and STUS schemes are equivalent for this problem. The STCS results shown in Figure 11 exhibit oscillation, with 0.009×10^7 ppt-ft^3 of material being diffused from cell (3,6). The results of the FTUS, FTCS, and FCT schemes are equivalent for this problem. Results shown in Figure 12 for the FCT scheme exhibit no oscillation and diffuse only 0.004×10^7 ppt-ft^3 of material from cell (3,6).

Time Step No. 10 Time = 1000.00 Concentration Field ($\times 10^3$)

M	N 1	2	3	4	5	6	7
1	0.	0.	0.	0.	0.	0.	0.
2	0.	-0.	0.	-0.	0.	-0.	0.
3	0.	0.	-0.	0.	-0.	0.	0.
4	0.	-0.	0.	-0.	0.	-0.	0.
5	0.	0.	-0.	0.	-0.	0.	0.
6	0.	-0.	1000.	-0.	0.	-0.	0.
7	0.	-0.	-0.	0.	-0.	0.	0.
8	0.	0.	0.	0.	0.	0.	0.

(STUS, STCS) Mass Grid Total 1.00000×10^7 ppt-ft^3

Figure 8. Stationary block problem (small grid case) STUS and STCS

Time Step No. 10 Time = 1000.00 Concentration Field ($\times 10^3$)

M	N 1	2	3	4	5	6	7
1	0.	0.	0.	0.	0.	0.	0.
2	0.	0.	0.	0.	0.	0.	0.
3	0.	0.	0.	0.	0.	0.	0.
4	0.	0.	0.	0.	0.	0.	0.
5	0.	0.	0.	0.	0.	0.	0.
6	0.	0.	1000.	0.	0.	0.	0.
7	0.	0.	0.	0.	0.	0.	0.
8	0.	0.	0.	0.	0.	0.	0.

(FTUS, FTCS, AND FCT) Mass Grid Total 1.00000×10^7 ppt-ft^3

Figure 9. Stationary block problem (small grid case) FTUS, FTCS, and FCT

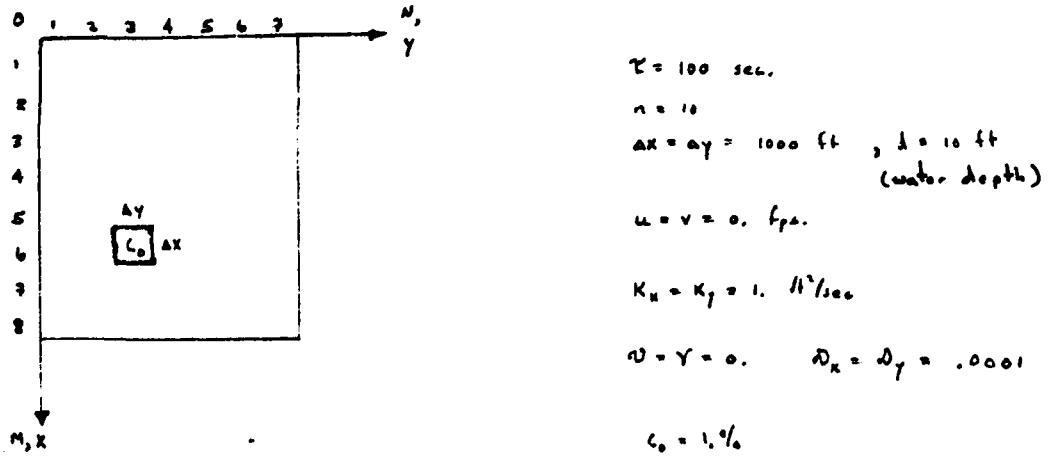

Figure 10. Diffusion of a block (small grid case)

Time Step No. 10 Time = 1000.00 Concentration Field ($\times 10^3$)

	N						
M	1	2	3	4	5	6	7
1	0.	0.	0.	0.	0.	0.	0.
2	0.	-0.	-0.	-0.	0.	-0.	0.
3	0.	0.	0.	0.	-0.	0.	0.
4	0.	-0.	-1.	-0.	0.	-0.	0.
5	0.	0.	3.	0.	-0.	0.	0.
6	0.	3.	991.	3.	-1.	0.	0.
7	0.	0.	3.	0.	-0.	0.	0.
8	0.	0.	0.	0.	0.	0.	0.

(STUS, STCS) Mass Grid Total 1.00088×10^7 ppt-ft^3

Figure 11. Diffusion of a block (small grid case) STUS and STCS

Time Step No. 10 Time = 1000.00 Concentration Field ($\times 10^3$)

	N						
M	1	2	3	4	5	6	7
1	0.	0.	0.	0.	0.	0.	0.
2	0.	0.	0.	0.	0.	0.	0.
3	0.	0.	0.	0.	0.	0.	0.
4	0.	0.	0.	0.	0.	0.	0.
5	0.	0.	1.	0.	0.	0.	0.
6	0.	1.	996.	1.	0.	0.	0.
7	0.	0.	1.	0.	0.	0.	0.
8	0.	0.	0.	0.	0.	0.	0.

(FTUS, FTCS, FCT) Mass Grid Total 0.999999×10^7 ppt-ft^3

Figure 12. Diffusion of a block (small grid case) FTUS, FTCS, and FCT

4. Front Translation Problem

Constituent concentration in cell (1,4) was initially set at 1 ppt and maintained at that level for 10 time-steps of 100-sec duration. The velocity was directed in the horizontal at a strength of 2 fps. No diffusion was considered. The problem setup is shown in Figure 13.

Over the 10 time-step run 2×10^7 ppt-ft^3 of mass is injected. Since each cell represents 10^7 ft^3 and the velocity magnitude is 2 fps,

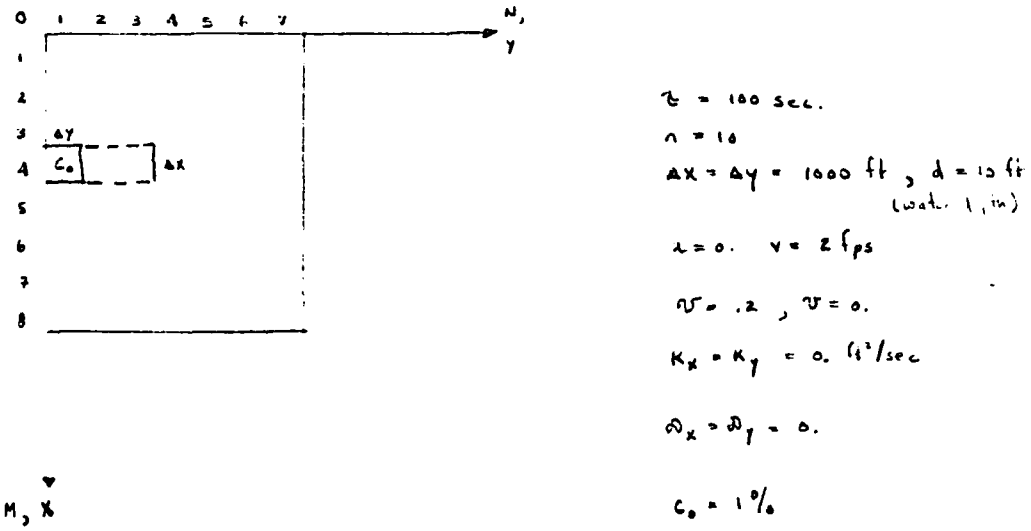

Figure 13. Front translation problem (small grid case)

cells (1,4), (2,4), and (3,4) should all be at 1 ppt strength at the end of the simulation.

The results for the FTUS scheme are shown in Figure 14. The

Time Step No. 10 Time = 1000.00 Concentration Field ($\times 10^3$)

	N						
M	1	2	3	4	5	6	7
1	0.	0.	0.	0.	0.	0.	0.
2	0.	0.	0.	0.	0.	0.	0.
3	0.	0.	0.	0.	0.	0.	0.
4	1000.	866.	594.	322.	142.	53.	0.
5	0.	0.	0.	0.	0.	0.	0.
6	0.	0.	0.	0.	0.	0.	0.
7	0.	0.	0.	0.	0.	0.	0.
8	0.	0.	0.	0.	0.	0.	0.

Mass Grid Total 2.97691×10^7 ppt-ft^3

Figure 14. FTUS front translation results

frontal smearing extends to the boundary of the 2×10^7 ppt-ft^3 mass injected and the 1×10^7 ppt-ft^3 initial mass, 2.97691×10^7 ppt-ft^3 remains in the systems, the remaining mass is lost through the boundary.

The results of the FCT scheme are shown in Figure 15. The frontal smearing is less severe for these schemes. Of the 2×10^7 ppt-ft^3

Time Step No. 10 Time = 1000.00 Concentration Field ($\times 10^3$)

	N						
M	1	2	3	4	5	6	7
1	0.	0.	0.	0.	0.	0.	0.
2	0.	0.	0.	0.	0.	0.	0.
3	0.	0.	0.	0.	0.	0.	0.
4	1000.	1000.	702.	226.	58.	9.	0.
5	0.	0.	0.	0.	0.	0.	0.
6	0.	0.	0.	0.	0.	0.	0.
7	0.	0.	0.	0.	0.	0.	0.
8	0.	0.	0.	0.	0.	0.	0.

Mass Grid Total 2.99515×10^7 ppt-ft^3

Figure 15. FCT front translation results

mass injected and the 1×10^7 ppt-ft^3 initial mass, 2.99515×10^7 ppt-ft^3 remains in the system, the remaining mass is lost through the boundary.

5. Rotation Problems

Consider the uniform rotation of strength ω (radian/sec) about cell (n_o,m_o) as shown in Figure 16. Define the following relations.

$$x' = (n - n_o)\Delta x$$

$$y' = (m - m_o)\Delta y$$

where

$m, n \equiv$ indices for cell (n,m)

$\Delta x, \Delta y \equiv$ grid spacings in the x and y directions, respectively

$m_o, n_o \equiv$ indices for rotation center

For an arbitrary cell (n,m), the velocity $\bar{v}$ is computed as follows.

$$\bar{v} = \bar{\omega} \times \bar{r} = \omega\hat{k} \times (x'\hat{i} + y'\hat{j}) = -\omega y'\hat{i} + \omega x'\hat{j}$$

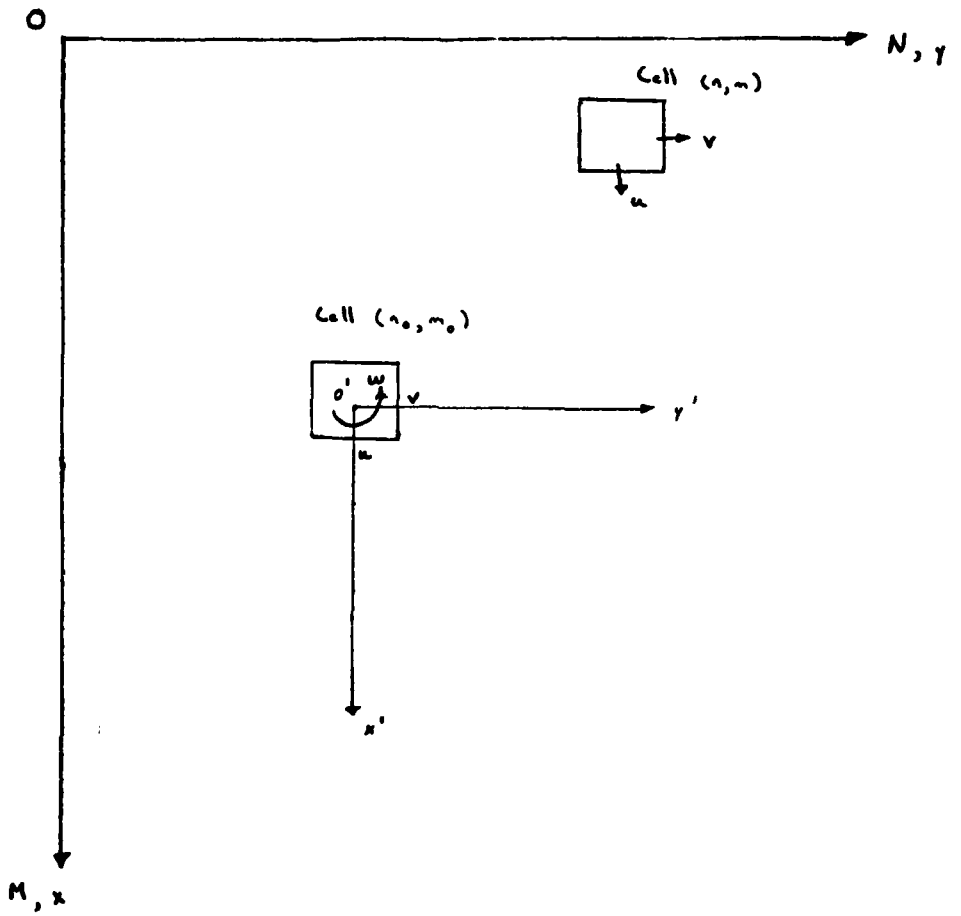

Figure 16. Rotation problem notation

Block rotation problem

A block of material initially occupying cell (3,3) at strength 1 ppt is rotated through 90° over 10 time steps of 100 second duration. At the end of this simulation, the block should occupy cell (5,5) at a strength of 1 ppt. The problem setup is shown in Figure 17.

The results of the FTUS are presented in Figure 18. The distribution is considerably smeared, with mass being lost through the

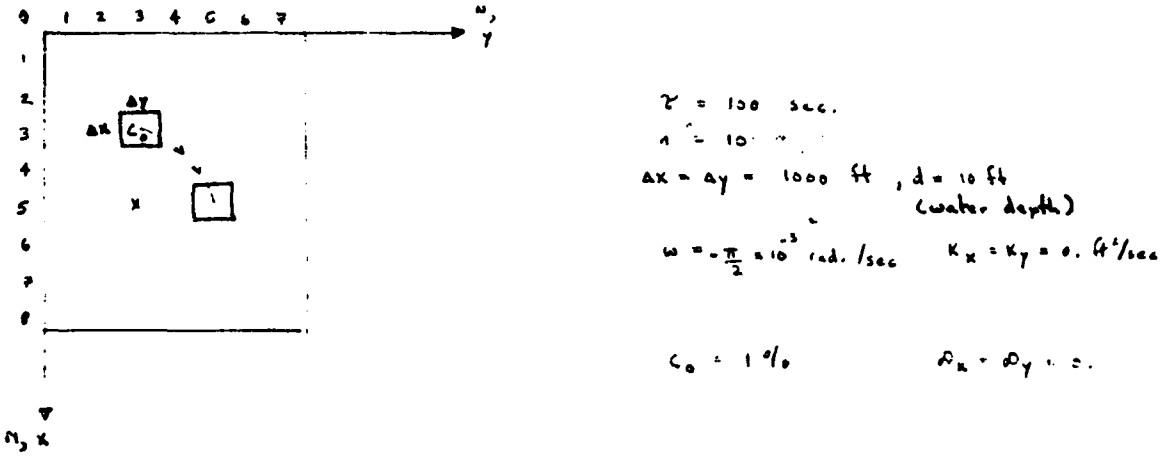

Figure 17. Rotation block problem (small grid case)

Time Step No. 10 Time = 1000.00 Concentration Field ($\times 10^3$)

	N						
M	1	2	3	4	5	6	7
1	0.	0.	0.	0.	0.	0.	0.
2	0.	0.	0.	0.	0.	0.	0.
3	0.	0.	42.	68.	54.	28.	0.
4	0.	0.	0.	68.	80.	49.	0.
5	0.	1.	0.	65.	81.	48.	0.
6	0.	4.	15.	40.	53.	32.	0.
7	0.	3.	9.	20.	26.	16.	0.
8	0.	0.	0.	0.	0.	0.	0.

Mass Grid Total 0.802150×10^7 ppt-ft^3

Figure 18. FTUS block rotation

boundaries. Of the original 1×10^7 ft^3-ppt of mass, 0.80215×10^7 ft^3-ppt remains on the computational grid.

The FCT scheme results are presented in Figure 19. The distribution is again smeared, with mass being lost through the boundaries. Of the original 1×10^7 ft^3-percent of mass, 0.878427×10^7 ft^3-percent remains on the computational grid. Thus, the FCT scheme is superior to the FTUS scheme in this regard.

Time Step No. 10 Time = 1000.00 Concentration Field ($\times 10^3$)

	N						
M	1	2	3	4	5	6	7
1	0.	0.	0.	0.	0.	0.	0.
2	0.	0.	0.	0.	0.	0.	0.
3	0.	0.	0.	148.	110.	14.	0.
4	0.	0.	-0.	95.	138.	64.	0.
5	0.	0.	0.	54.	103.	48.	0.
6	0.	1.	4.	21.	39.	16.	0.
7	0.	0.	1.	5.	8.	2.	0.
8	0.	0.	0.	0.	0.	0.	0.

Mass Grid Total 0.878427×10^7 ppt-ft^3

Figure 19. FCT block rotation

Front rotation

Constituent concentration in cell (1,4) was initially set at 1 ppt and maintained at that level for 10-time steps of 100-sec duration. A circular velocity field at the center of cell (1,7) was specified such that the front would rotate and occupy cell (4,7) at the end of the simulation. The problem setup is shown in Figure 20.

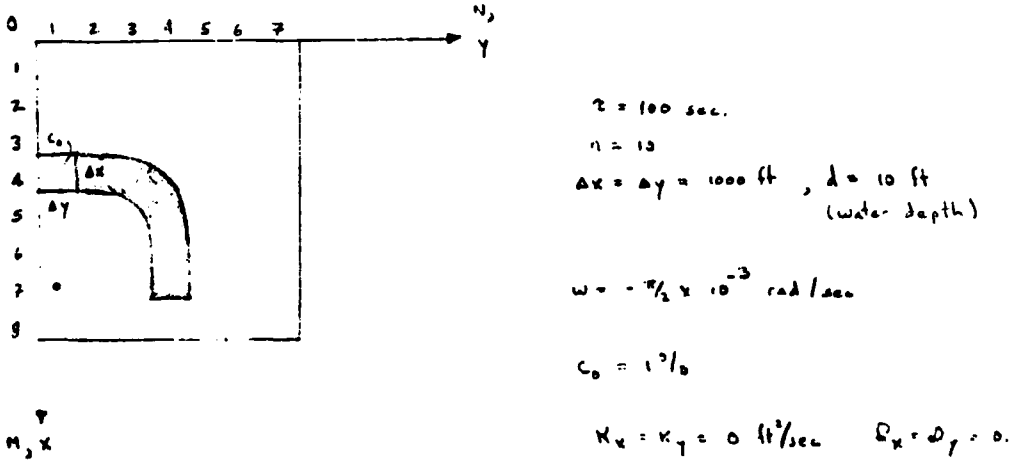

Figure 20. Front rotation problem (small grid case)

Over the 10 time-step run 4.7124×10^7 ft^3-ppt of mass is injected. Since each cell represents 10^7 ft^3 and considering boundary input cell (1,4), the total grid mass should equal 5.7124×10^7 ppt-ft^3.

The results for the FTUS scheme are shown in Figure 21. Frontal smearing extends to the boundary resulting in a grid mass total of 4.82762×10^7 ppt-ft^3.

The results of the FCT scheme are shown in Figure 22. Frontal smearing is less severe in this scheme with a mass grid total of 5.22026×10^7 ppt-ft^3.

Time Step No. 10 Time = 1000.00 Concentration Field ($\times 10^3$)

	N						
M	1	2	3	4	5	6	7
1	0.	0.	0.	0.	0.	0.	0.
2	0.	0.	0.	0.	0.	0.	0.
3	0.	0.	0.	0.	0.	0.	0.
4	1000.	749.	447.	221.	93.	34.	0.
5	0.	243.	332.	254.	139.	60.	0.
6	0.	102.	221.	215.	136.	65.	0.
7	0.	50.	148.	160.	107.	52.	0.
8	0.	0.	0.	0.	0.	0.	0.

Mass Grid Total 4.82762×10^7 ppt-ft^3

Figure 21. FTUS front rotation

Time Step No. 10 Time = 1000.00 Concentration Field ($\times 10^3$)

	N						
M	1	2	3	4	5	6	7
1	0.	0.	0.	0.	0.	0.	0.
2	0.	0.	0.	0.	0.	0.	0.
3	0.	0.	0.	0.	0.	0.	0.
4	1000.	933.	587.	197.	23.	-0.	0.
5	0.	108.	511.	424.	187.	30.	0.
6	0.	13.	273.	333.	203.	65.	0.
7	0.	11.	93.	121.	79.	28.	0.
8	0.	0.	0.	0.	0.	0.	0.

Mass Grid Total 5.22026×10^7 ppt-ft^3

Figure 22. FCT front rotation

6. Summary of Small Grid Test Results

By employing a 7 × 8 grid, it was possible to verify the computational schemes. Due to the grid size boundary effects influenced the computations for the majority of the problems considered.

The FCT method proved to be the superior technique for the block translation problem, since the mass lost through the boundary was less for this scheme than for all other schemes.

For the block diffusion problem, simulation results were the same for FCT, FTCS, and FTUS schemes. This result is expected, since in the absence of advection the FTCS and FTUS schemes are equivalent. The STCS scheme exhibit minor oscillations in the solution surface. This result is somewhat unexpected.

In both the block and front rotation problems, the FCT scheme proved superior to the FTUS scheme in terms of minimizing mass lost through the computational boundaries.

PART IV: LARGE GRID (60 × 60) TEST RESULTS

A 60 × 60 computational grid was constructed to perform additional testing. All work in this phase was conducted on the Boeing Computer Services CRAY-IA in Renton, Washington. The problems considered and scheme results are presented in turn below.

1. Single Cell Block Translation

The same problem considered in the small grid setting was setup as shown in Figure 23. The initial unit concentration in cell (30,30) was to be advected to cell (32,28) over ten time steps of 100 second duration.

The results for the FCT scheme are shown in Figure 24. We note the symmetry about the diagonal (the direction of translation). All mass is preserved; i.e., no mass is lost through the boundaries.

2. Single Cell Block Diffusion

The diffusion of a unit concentration initially in cell (30,30) is considered as shown in Figure 25 for 10 time steps of 100 second duration. Diffusion coefficients are increased from 1 ft/sec of the previous small grid to 100 ft^2/sec.

The results of the FCT scheme are shown in Figure 26. Since $K_x = K_y$, the results are symmetrical in the x and y axes. No mass is lost through the boundaries. The computed results are compared with the analytical solution results in Table III. The computed results represent values over an entire grid cell area of 10^6 ft^2, whereas the analytical results correspond to the point value at the center of each cell. As $\Delta t, \Delta x, \Delta y \to 0$, the computed results should approach the analytical value.

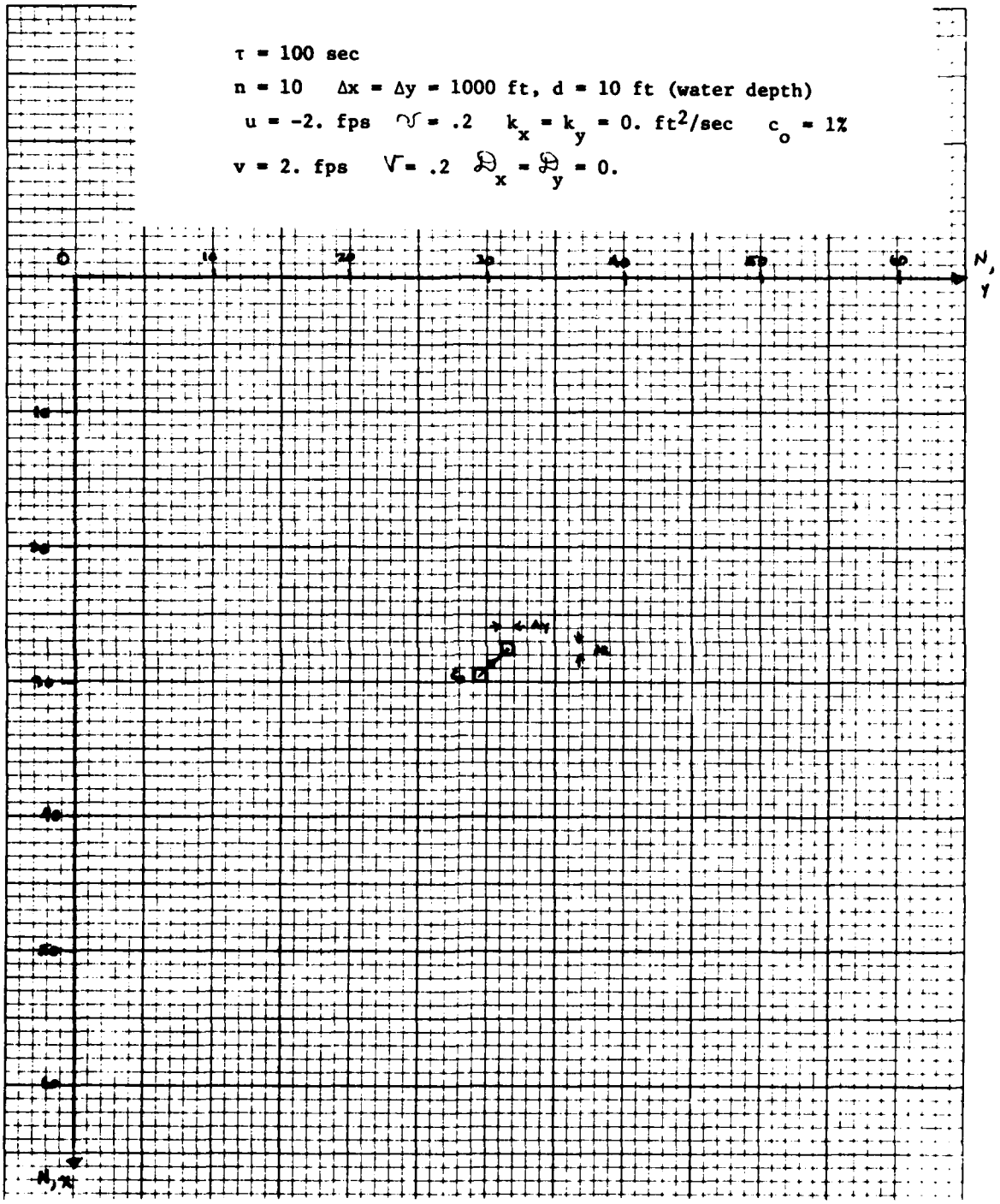

Figure 23. Single cell block translation (large grid case)

	N										
M	27	28	29	30	31	32	33	34	35	36	37
22	0.	0.	0.	0.	0.	0.	0.	0.	0.	0.	0.
23	0.	0.	0.	0.	0.	0.	0.	0.	0.	0.	0.
24	0.	0.	0.	0.	1.	0.	0.	0.	0.	0.	0.
25	0.	0.	0.	1.	3.	2.	1.	0.	0.	0.	0.
26	0.	0.	0.	4.	15.	10.	4.	1.	0.	0.	0.
27	0.	0.	0.	14.	51.	35.	13.	4.	1.	0.	0.
28	0.	0.	0.	35.	127.	90.	35.	10.	2.	0.	0.
29	0.	0.	0.	59.	162.	127.	51.	15.	3.	1.	0.
30	0.	0.	0.	8.	59.	35.	14.	4.	1.	0.	0.
31	0.	0.	0.	0.	0.	0.	0.	0.	0.	0.	0.
32	0.	0.	0.	0.	0.	0.	0.	0.	0.	0.	0.
33	0.	0.	0.	0.	0.	0.	0.	0.	0.	0.	0.

Figure 24. FCT block translation (large grid case) ($\times 10^3$)

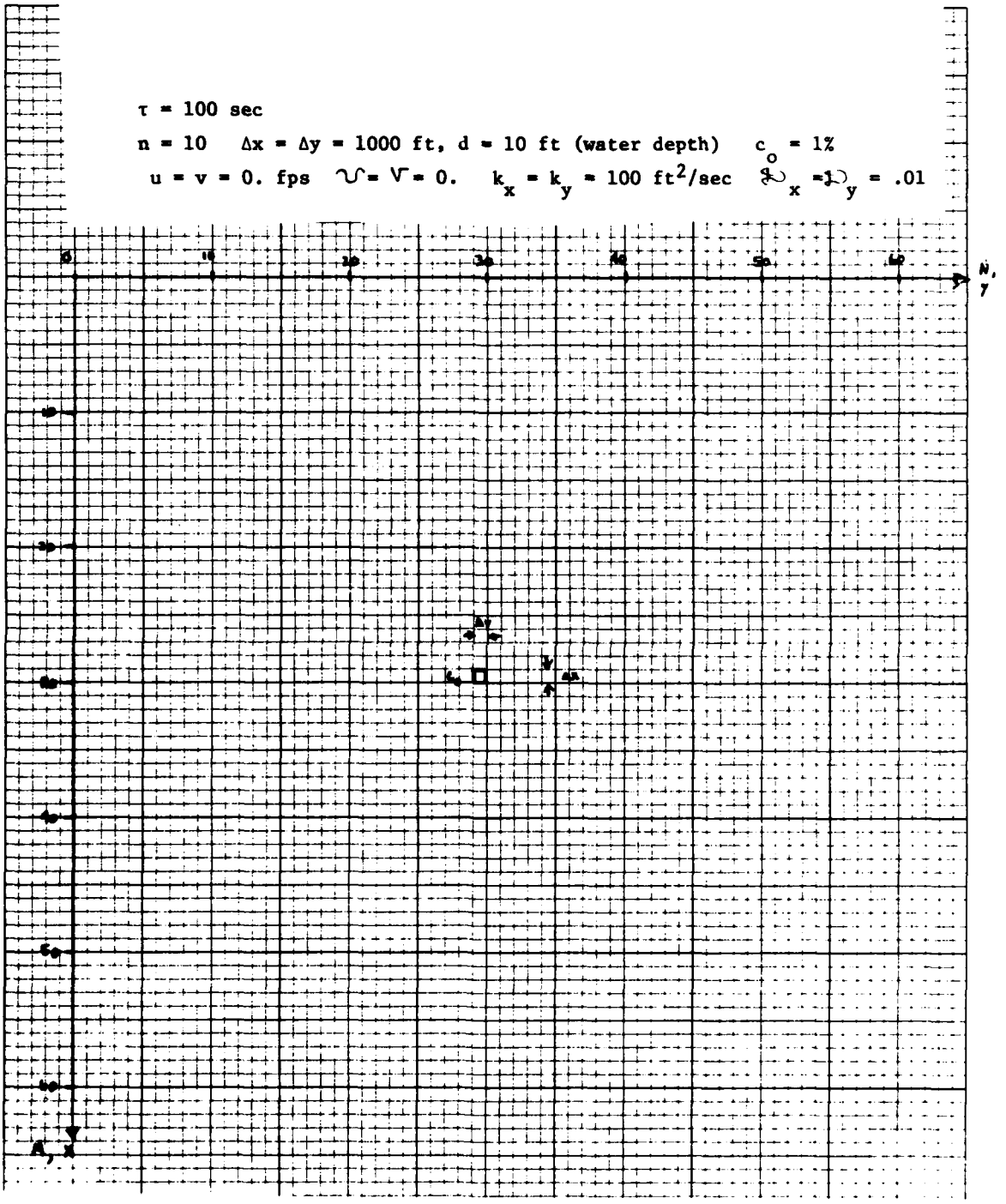

Figure 25. Single cell block diffusion (large grid case)

	N								
M	26	27	28	29	30	31	32	33	34
25	0.	0.	0.	0.	0.	0.	0.	0.	0.
26	0.	0.	0.	0.	0.	0.	0.	0.	0.
27	0.	0.	0.	0.	0.	0.	0.	0.	0.
28	0.	0.	0.	0.	3.	0.	0.	0.	0.
29	0.	0.	0.	7.	68.	7.	0.	0.	0.
30	0.	0.	3.	68.	684.	68.	3.	0.	0.
31	0.	0.	0.	7.	68.	7.	0.	0.	0.
32	0.	0.	0.	0.	3.	0.	0.	0.	0.
33	0.	0.	0.	0.	0.	0.	0.	0.	0.
34	0.	0.	0.	0.	0.	0.	0.	0.	0.
35	0.	0.	0.	0.	0.	0.	0.	0.	0.
36	0.	0.	0.	0.	0.	0.	0.	0.	0.

Figure 26. FCT diffusion (large grid case) ($\times 10^3$)

Table III. Single Cell Block Diffusion Simulation Versus Analytical Solution Comparison

Location	Analytical Result	Computed Result
(30,30)	0.7768	0.684
(31,30)	0.1018	0.068
(32,30)	0.0003	0.003
(31,29)	0.0172	0.007

3. Multicell Block Translation

For this problem $\Delta x = \Delta y = 100$ ft, and $\Delta t = 10$ seconds as shown in Figure 27. 100 cells were used to represent the same distribution represented by one cell in the single cell problem. In order to reduce computational costs, 50 time-steps were employed.

The FCT scheme results at the end of 50 time-steps are presented in Figure 28. Note again the symmetry about the streamline. No mass was lost through the boundary and no oscillations were present in the solution. All material in the multicell block translation problem is contained within an area equal to that of 6 cells of the single block translation simulation, while in that simulation the original distribution was spread over 19 cells. Thus by reducing the time- and space-steps a more accurate result is obtained.

The STCS scheme results at the end of 50 time-steps are presented in Figure 29. Oscillations developed behind the front and spread to the boundary, essentially destroying the solution. Mass appeared to be created through the first 37 time-steps and destroyed over the last 13 time-steps.

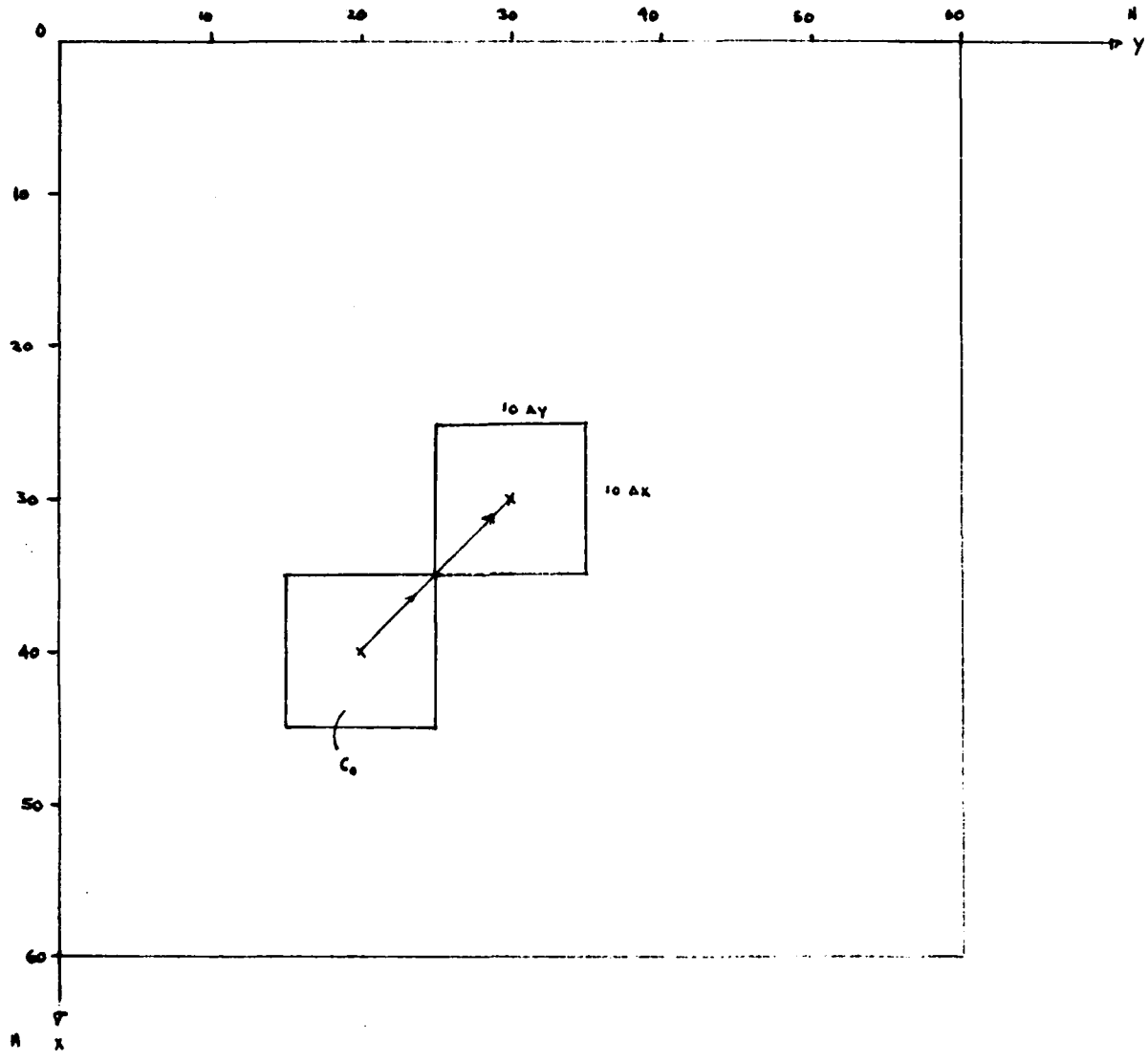

n_x = 10 cells
n_y = 10 cells
$|u| = |v|$ = 2 fps
$\Delta x = \Delta y$ = 100 ft
τ = 10 sec.
n = 50
$\sqrt{}$ = .2
$\sqrt{}$ = .2
c_o = 1 ppt
d = 10 ft (water depth)

Figure 27. Multicell block translation (large grid case)

M	N																			
	21	22	23	24	25	26	27	28	29	30	31	32	33	34	35	36	37	38	39	40
24	0.	0.	0.	2.	47.	96.	116.	118.	120.	144.	171.	173.	142.	99.	59.	31.	14.	6.	2.	1.
25	0.	0.	0.	18.	100.	194.	238.	245.	252.	297.	349.	353.	294.	206.	124.	66.	31.	13.	5.	2.
26	0.	0.	0.	38.	190.	349.	437.	456.	477.	550.	635.	643.	542.	383.	233.	124.	59.	25.	10.	4.
27	0.	0.	0.	70.	323.	553.	686.	755.	823.	901.	977.	993.	885.	625.	383.	206.	99.	43.	17.	6.
28	0.	0.	0.	111.	478.	765.	934.	1000.	1000.	1000.	1000.	1000.	1000.	885.	542.	294.	142.	63.	25.	9.
29	0.	0.	0.	148.	536.	912.	991.	996.	998.	999.	999.	1000.	1000.	993.	643.	353.	173.	76.	31.	12.
30	0.	0.	0.	155.	618.	816.	916.	964.	983.	992	997.	999.	1000.	977.	635.	349.	171.	76.	31.	12.
31	0.	0.	0.	122.	419.	659.	826.	916.	957.	579.	992.	999.	1000.	901.	550.	297.	144.	63.	25.	9.
32	0.	0.	0.	13.	314.	602.	791.	886.	928.	957.	983.	998.	1000.	823.	477.	252.	120.	52.	21.	8.
33	0.	0.	0.	36.	366.	644.	808.	868.	886.	916.	964.	996.	1000.	755.	456.	246.	118.	51.	20.	7.
34	0.	0.	0.	105.	422.	666.	786.	808.	791.	826.	916.	991.	934.	696.	437.	238.	116.	52.	21.	8.
35	0.	0.	0.	70.	312.	544.	666.	644.	682.	659.	816.	912.	765.	553.	349.	194.	96.	43.	18.	7.
36	0.	0.	0.	0.	73.	312.	422.	366.	314.	419.	618.	596.	478.	323.	190.	100.	47.	20.	8.	3.
37	0.	0.	1.	0.	0.	70.	105.	36.	13.	122.	155.	148.	111.	70.	38.	18.	8.	3.	1.	0.
38	0.	0.	5.	1.	0.	0.	0.	0.	0.	0.	0.	0.	0.	0.	0.	0.	0.	0.	0.	0.
39	0.	3.	0.	0.	0.	0.	0.	0.	0.	0.	0.	0.	0.	0.	0.	0.	0.	0.	0.	0.
40	0.	0.	0.	0.	0.	0.	0.	0.	0.	0.	0.	0.	0.	0.	0.	0.	0.	0.	0.	0.
41	0.	0.	0.	0.	0.	0.	0.	0.	0.	0.	0.	0.	0.	0.	0.	0.	0.	0.	0.	0.
42	0.	0.	0.	0.	0.	0.	0.	0.	0.	0.	0.	0.	0.	0.	0.	0.	0.	0.	0.	0.
43	-0.	-0.	0.	0.	0.	0.	0.	0.	0.	0.	0.	0.	0.	0.	0.	0.	0.	0.	0.	0.
44	0.	-0.	-0.	-0.	-0.	-0.	-0.	-0.	0.	0.	0.	0.	0.	0.	0.	0.	0.	0.	0.	0.
45	-0.	-0.	0.	0.	0.	-0.	0.	0.	0.	0.	0.	0.	0.	0.	0.	0.	0.	0.	0.	0.

Figure 28. FCT block translation (large grid case) ($\times 10^3$)

	N																			
M	21	22	23	24	25	26	27	28	29	30	31	32	33	34	35	36	37	38	39	40
16	-0.	-0.	0.	0.	-0.	-0.	-0.	-0.	-0.	-0.	-0.	-0.	-0.	-0.	-0.	-0.	-0.	0.	0.	-0.
17	0.	0.	-0.	-0.	0.	0.	0.	0.	0.	0.	0.	0.	0.	0.	0.	0.	0.	-0.	-0.	0.
18	-0.	-0.	0.	0.	-0.	-0.	-0.	-0.	-0.	-0.	-0.	-0.	-0.	-0.	-0.	-0.	-0.	0.	0.	-0.
19	-0.	-0.	0.	0.	-0.	-0.	-0.	-0.	-0.	-0.	-0.	-0.	-0.	-0.	-0.	-0.	-0.	0.	0.	-0.
20	0.	0.	-0.	-0.	0.	0.	0.	0.	0.	0.	0.	0.	0.	0.	0.	0.	0.	-0.	-0	0.
21	0.	0.	-0.	-0.	0.	1.	1.	1.	1.	1.	1.	1.	1.	1.	1.	0.	0.	-0.	-0.	0.
22	-0.	-0.	0.	0.	-1.	-2.	-2.	-2.	-2.	-2.	-2.	-2.	-2.	-2.	-1.	-0.	-0.	0.	0.	-0.
23	-3.	-0.	2.	1.	-4.	-13.	-16.	-13.	-15.	-17.	-13.	-13.	-17.	-17.	-10.	-3.	-0.	0.	0.	-0.
24	0.	0.	-0.	-0.	1.	2.	2.	2.	2.	2.	2.	2.	2.	2.	1.	0.	0.	-0.	-0.	0.
25	32.	5.	-27.	-13.	49.	161.	201.	171.	193.	212.	171.	170.	222.	213.	123.	36.	0.	-3.	-0.	0.
26	109.	16.	-93.	-44.	167.	552.	688.	586.	661.	724.	583.	580.	757.	728.	419.	123.	1.	-10.	-1.	1.
27	190.	28.	-162.	-76.	290.	857.	1184.	1017.	1147.	1255.	1012.	1007.	1314.	1262.	728.	213.	2.	-17.	-2.	1.
28	198.	30.	-169.	-78.	302.	996.	1242.	1058.	1183.	1306.	1053.	1048.	1367.	1314.	757.	222.	2.	-17.	-2.	1.
29	151.	22.	-129.	-60.	231.	763.	552.	811.	915.	1001.	807.	803.	1048.	1007.	580.	170.	2.	-13.	-2.	1.
30	152.	23.	-130.	-61.	233.	767.	957.	815.	919.	1006.	811.	807.	1053.	1012.	583.	171.	2.	-13.	-2.	1.
31	189.	28.	-161.	-75.	288.	952.	1187.	1011.	1140.	1248.	1006.	1001.	1306.	1255.	724.	212.	2.	-17.	-2.	1.
32	173.	26.	-147.	-69.	263.	870.	1085.	924.	1042.	1140.	919.	915.	1193.	1147.	661.	193.	2.	-15.	-2.	1.
33	153.	23.	-131.	-61.	234.	771.	962.	819.	924.	1011.	815.	811.	1058.	1017.	586.	171.	2.	-13.	-2.	1.
34	180.	27.	-153.	-71.	274.	905.	1129.	962.	1085.	1187.	957.	952.	1242.	1194.	688.	201.	2.	-16.	-2.	1.
35	144.	22.	-123.	-57.	220.	726.	805.	771.	870.	952.	767.	763.	996.	957.	552.	161.	2.	-13.	-2.	1.
36	44.	7.	-37.	-17.	67.	220.	274.	234.	263.	288.	233.	231.	302.	290.	167.	49.	1.	-4.	-1.	0.
37	-11.	-2.	10.	5.	-17.	-57.	-71.	-61.	-69.	-75.	-61.	-60.	-79.	-76.	-44.	-13.	-0.	1.	0.	-0.
38	-24.	-4.	21.	10.	-37.	-123.	-153.	-131.	-147.	-161.	-130.	-129.	-169.	-162.	-93.	-27.	-0.	2.	0.	-0.
39	4.	1.	-4.	-2.	7.	22.	27.	23.	26.	28.	23.	23.	30.	28.	16.	5.	0.	-0.	-0.	0.
40	29.	4.	-24.	-11.	44.	144.	180.	153.	173.	189.	152.	151.	198.	190.	109.	32.	0.	-3.	-0.	0.
41	-22.	-3.	19.	9.	-34.	-113.	-141.	-120.	-135.	-148.	-120.	-119.	-155.	-149.	-86.	-25.	-0.	2.	0.	-0.
42	-11.	-2.	9.	4.	-17.	-55.	-69.	-58.	-66.	-72.	-58.	-58.	-75.	-72.	-42.	-12.	-0.	1.	0.	-0.
43	31.	5.	-27.	-12.	47.	157.	196.	167.	188.	206.	166.	165.	215.	207.	119.	35.	0.	-3.	-0.	0.
44	-21.	-3.	18.	8.	-32.	-106.	-132.	-112.	-127.	-139	-112.	-111.	-145.	-140.	-80.	-24.	-0.	2.	0.	-0.
45	-4.	-1.	4.	2.	-7.	-22.	-28.	-23.	-26.	-29.	-23.	-23.	-30.	-29.	-17.	-5.	-0.	0.	0.	-0.

Figure 29. STCS block translation (large grid case) ($\times 10^3$)

4. Multicell Front Translation

For this purpose the spatial step is 100 ft and the time step is 10 seconds as shown in Figure 30. Constituent concentration in cells (1,26)-(1,35) was set initially at 1 ppt and maintained at that level for 50 time-steps. The velocity was directed in the horizontal at 2 fps. No diffusion was considered.

Over the 50-time-step run 100×10^5 ppt-ft^3 of mass is injected. Since each cell represents 10^5 ft^3, the sum of the cell concentrations at the end of the simulation should equal 110 ppt-ft^3 (100 ppt-ft^3 due to injection and 10 from the boundary condition). The results of the FCT scheme shown in Figure 31 completely preserve mass. Since the horizontal velocity is 2 fps, at the end of the simulation all concentrations in the rectangular area (1,26)-(1,35), (11,26)-(11,25) should be equal to 1 ppt. As shown in Figure 31, the FCT scheme exhibits some frontal smearing.

This problem demonstrated the ability of the FCT scheme to preserve mass for injection (source) type problems.

5. Summary of Large Grid Test Results

The FCT scheme preserves mass. No mass was lost through the computational boundaries in either the single advection or diffusion problems. The multicell advection (block translation) problem demonstrated that by reducing the time and space steps, the FCT scheme will produce a more accurate result. The STCS scheme results for this problem exhibited severe oscillations behind the front eventually destroying the solution. The multicell front translation problem demonstrated the ability of the FCT scheme to handle injection- (source-) type problems.

Based upon these additional tests in conjunction with the small grid test results, the FCT scheme was selected for incorporation in the Waterways Experiment Station Implicit Flooding Model (WIFM).

τ = 10.0 sec

n = 50 $\Delta x = \Delta y$ = 100 ft, d = 10 ft (water depth)

$|u| = 0.$ $|v|$ = 2 fps $k_x = k_y = 0.$ ft^2/sec $\mathfrak{D}_x = \mathfrak{D}_y = 0.$

$U = \frac{|u|\,\Delta t}{\Delta x} = 0.$ $V = \frac{|v|\,\Delta t}{\Delta y} = .2$ c_o = 1 ppt

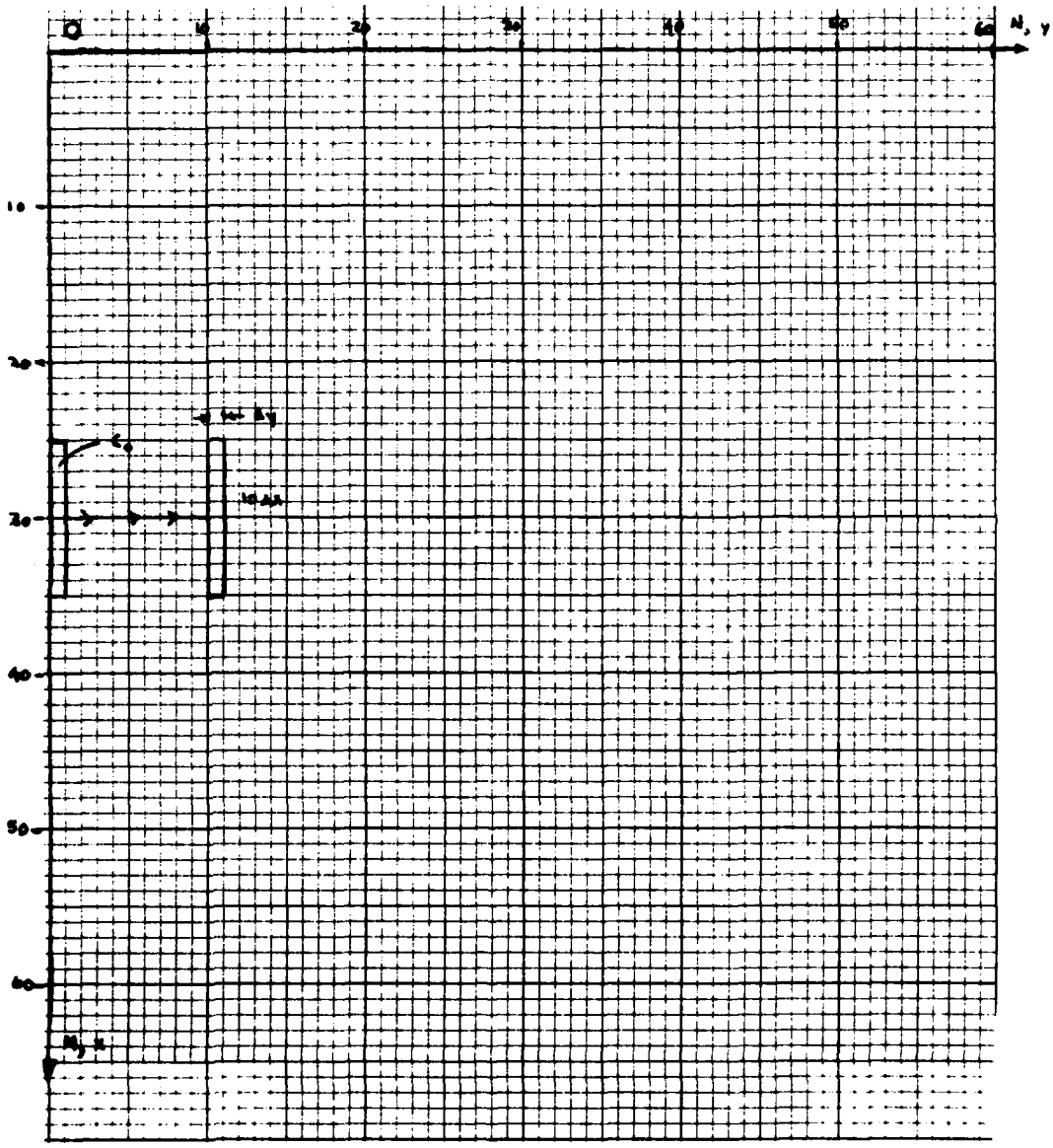

Figure 30. Multicell front translation (large grid case)

	N																		
M	1	2	3	4	5	6	7	8	9	10	11	12	13	14	15	16	17	18	19
24	0.	0.	0.	0.	0.	0.	0.	0.	0.	0.	0.	0.	0.	0.	0.	0.	0.	0.	0.
25	0.	0.	0.	0.	0.	0.	0.	0.	0.	0.	0.	0.	0.	0.	0.	0.	0.	0.	0.
26	1000.	1000.	1000.	1000.	1000.	1000.	1000.	1000.	1000.	912.	551.	295.	142.	62.	25.	9.	3.	1.	0.
27	1000.	1000.	1000.	1000.	1000.	1000.	1000.	1000.	1000.	912.	551.	295.	142.	62.	25.	9.	3.	1.	0.
28	1000.	1000.	1000.	1000.	1000.	1000.	1000.	1000.	1000.	912.	551.	295.	142.	62.	25.	9.	3.	1.	0.
29	1000.	1000.	1000.	1000.	1000.	1000.	1000.	1000.	1000.	912.	551.	295.	142.	62.	25.	9.	3.	1.	0.
30	1000.	1000.	1000.	1000.	1000.	1000.	1000.	1000.	1000.	912.	551.	295.	142.	62.	25.	9.	3.	1.	0.
31	1000.	1000.	1000.	1000.	1000.	1000.	1000.	1000.	1000.	912.	551.	295.	142.	62.	25.	9.	3.	1.	0.
32	1000.	1000.	1000.	1000.	1000.	1000.	1000.	1000.	1000.	912.	551.	295.	142.	62.	25.	9.	3.	1.	0.
33	1000.	1000.	1000.	1000.	1000.	1000.	1000.	1000.	1000.	912.	551.	295.	142.	62.	25.	9.	3.	1.	0.
34	1000.	1000.	1000.	1000.	1000.	1000.	1000.	1000.	1000.	912.	551.	295.	142.	62.	25.	9.	3.	1.	0.
35	1000.	1000.	1000.	1000.	1000.	1000.	1000.	1000.	1000.	912.	551.	295.	142.	62.	25.	9.	3.	1.	0.
36	0.	0.	0.	0.	0.	0.	0.	0.	0.	0.	0.	0.	0.	0.	0.	0.	0.	0.	0.
37	0.	0.	0.	0.	0.	0.	0.	0.	0.	0.	0.	0.	0.	0.	0.	0.	0.	0.	0.

Figure 31. FCT multicell front translation (large grid cell) ($\times 10^3$)

PART V: VARIABLE GRID TESTING ON THE MISSISSIPPI SOUND GLOBAL GRID

The FCT algorithm was incorporated as a group of subroutines in the WIFM to simulate salinity. Density coupling was not considered. Since the numerical investigation of Mississippi Sound is concerned only with fixed boundary problems, the flooding routine was removed from WIFM. The resulting hydrodynamic-salinity code (WIFM-SAL) enables the treatment of the general fixed boundary nonlinear problem on a variably stretched grid. The exponentially stretched grid shown in Figure 32 employing 6785 computational cells with a minimum spatial resolution of approximately 4000 feet has been developed to describe global circulation and horizontal salinity variation in Mississippi Sound.

In order to describe the dispersion mechanics within Mississippi Sound the following relations are employed in WIFM-SAL.

$$K_x = D\sqrt{g}\,\frac{|u|h}{C} + K_x' \qquad (5.1)$$

$$K_y = D\sqrt{g}\,\frac{|v|h}{C} + K_y'$$

where

K_x, K_y ≡ dispersion coefficients (ft^2/sec)

D ≡ dimensionless constant (5.93-20.2) in the direction of flow 0.23 in the direction perpendicular to flow

C ≡ Chezy coefficient (dimensions of $\sqrt{g}$)

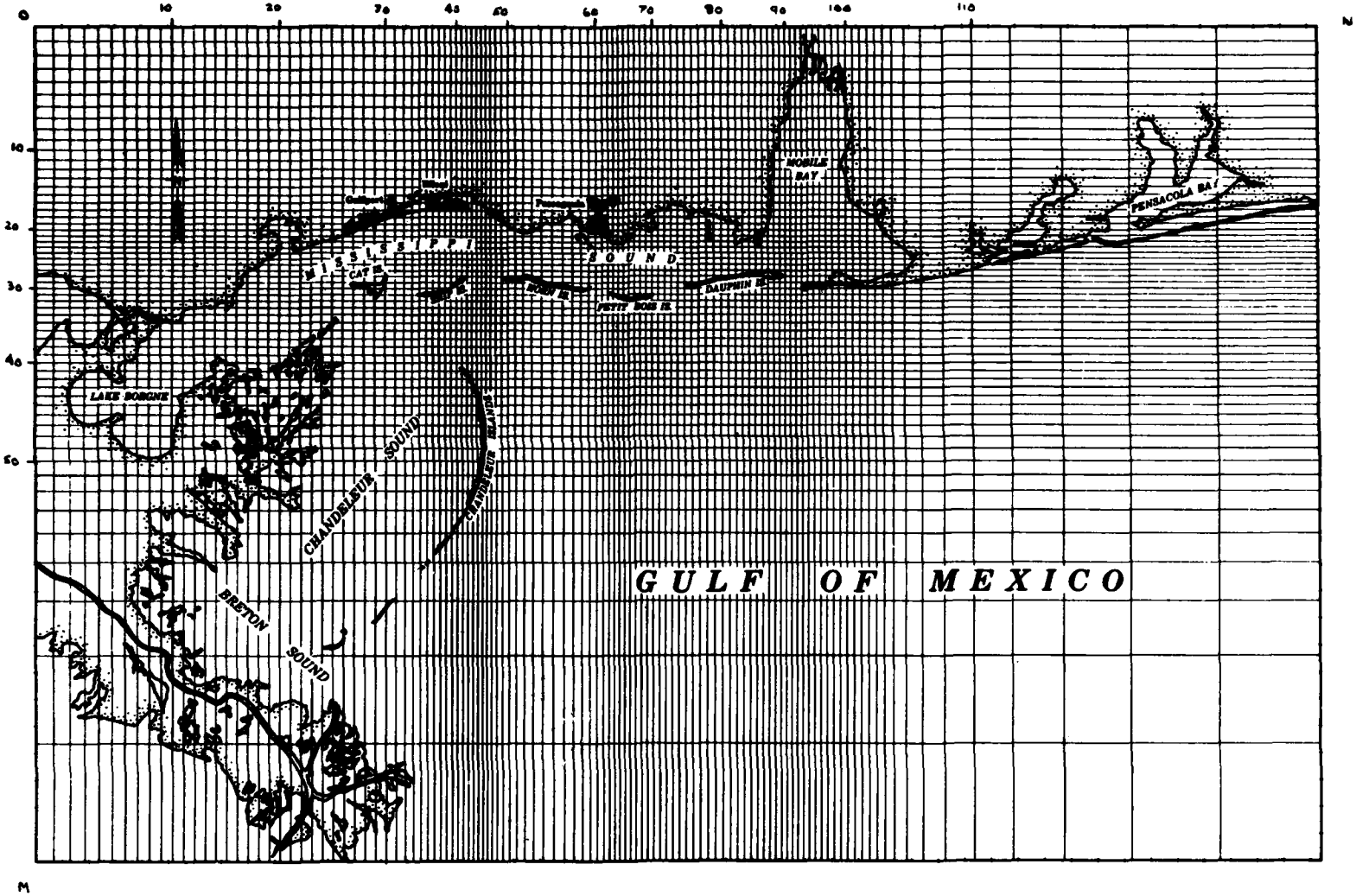

Figure 32. Mississippi Sound global grid

$g \equiv$ gravity (ft/sec^2)

$h \equiv$ water depth digitized over the global grid (ft)

$u, v \equiv$ velocity components in the x and y directions, respectively fps

$K'_x, K'_y \equiv$ additional dispersion effects (ft^2/sec)

As in the testing on the regularly spaced grids the following sharp front problem was considered. The hydrodynamic problem setup employed initial water surface elevations set to zero over the computational domain, flow inputs of 4 ft^2/sec per unit flow width at cells (97,3) and (2,44), and a ramp function of 1/6 ft per time-step.

The salinity problem setup employed initial zero concentration levels over the entire computational region except in a block of ten cells as shown below.

$$S^o_{n,m} = \begin{cases} 0.0 \text{ ppt} & n \notin (101,105) \\ & m \notin (54,55) \\ 10.0 \text{ ppt} & n \in (101,105) \\ & m \in (54,55) \end{cases} \qquad (5.2)$$

Salinity levels were maintained at zero at the two flow input locations. In the dispersion relations, $c_x = c_y = 10.0$ and $K'_x = K'_y = 0.0$ ft^2/sec. A 5 time-step simulation was performed employing a time-step length of 6 minutes for several numerical schemes.

In order to characterize the transport characteristics of these simulations the following dimensionless numbers may be considered.

$$Cr^k_{x_{n,m}} = \frac{\left|u^k_{n,m+1/2}\right|\Delta t}{(\mu_1)_m \Delta\alpha_1} \qquad Cr^k_{y_{n,m}} = \frac{\left|v^k_{n+1/2,m}\right|\Delta t}{(\mu_2)_n \Delta\alpha_2} \tag{5.3}$$

$$Pe^k_{x_{n,m}} = \frac{\left|u^k_{n,m+1/2}\right|(\mu_1)_m \Delta\alpha_1}{K^k_{xn,m+1/2}} \qquad Pe^k_{y_{n,m}} = \frac{\left|v^k_{n+1/2,m}\right|(\mu_2)_n \Delta\alpha_2}{K^k_{yn+1/2,m}} \tag{5.4}$$

where

$Cr^k_{x_{n,m}}$ ≡ x - α_1 cell (n,m) particle velocity Courant number at time k

$Cr^k_{y_{n,m}}$ ≡ y - α_2 cell (n,m) particle velocity Courant number at time k

$Pe^k_{x_{n,m}}$ ≡ x - α_1 cell (n,m) Peclet number at time k

$Pe^k_{y_{n,m}}$ ≡ y - α_2 cell (n,m) Peclet number at time k

Δt ≡ time-step length

$\Delta\alpha_1$ ≡ α_1 space increment

$\Delta\alpha_2$ ≡ α_2 space increment

$(\mu_1)_m$ ≡ cell (n,m) stretching coefficient in the α_1 direction

$(\mu_2)_n$ ≡ cell (n,m) stretching coefficient in the α_2 direction

$u^k_{n,m+1/2}$ ≡ velocity component in cell (n,m) at time k in the α_1 direction

$v^k_{n+1/2,m}$ ≡ velocity component in cell (n,m) at time k in the α_2 direction

$K^k_{xn,m+1/2}$ ≡ dispersion coefficient in cell (n,m) at time in the α_1 direction

$K^k_{yn+1/2,m}$ ≡ dispersion coefficient in cell (n,m) at time in the α_2 direction

In general, these dimensionless numbers vary in time as well as in space over the computational grid and time interval of concern. Normal practice is to replace the time dependency of the cell velocity components by their maximum values, thus removing the time dependency. In all simulations, the following relations for the cell particle velocity Courant numbers hold.

$$Cr^k_{x_{n,m}}\ ,\quad Cr^k_{y_{n,m}} \leq 0.3 \tag{5.5}$$

The time dependency in the Peclet numbers, may be removed by substituting (5.1) into (5.4) with $K'_x = K'_y = 0.0$ ft^2/sec. Thus obtain for $Pe^k_{x_{n,m}}$ (results for $Pe^k_{y_{n,m}}$ are analogous).

$$Pe^k_{x_{n,m}} = \frac{\left|u^k_{n,m+1/2}\right|(\mu_1)_m\Delta\alpha_1}{D\sqrt{g}\left|u^k_{n,m+1/2}\right|h^k_{n,m}/c^k_{n,m}} = \frac{c^k_{n,m}(\mu_1)_m\Delta\alpha_1}{D\sqrt{g}h^k_{n,m}} \tag{5.6}$$

Since $c^k_{n,m}$ and $h^k_{n,m}$ vary extremely slowly with time, we may drop the k superscript and obtain

$$Pe_{x_{n,m}} = \frac{c_{n,m}(\mu_1)_m\Delta\alpha_1}{D\sqrt{g}h_{n,m}} \qquad Pe_{y_{n,m}} = \frac{c_{n,m}(\mu_2)_n\Delta\alpha_2}{D\sqrt{g}h_{n,m}} \tag{5.7}$$

In all simulations, the following relations hold for the cell Peclet numbers in the vicinity of the sharp front:

$$Pe_{x_{n,m}}\ ,\quad Pe_{y_{n,m}} \geq 100 \tag{5.8}$$

Results at the end of the simulation for the FTUS scheme are shown in Figure 33. All concentrations are positive and the initial mass of 0.132435×10^{14} ppt-ft^3 equaled the final mass plus the diffusion of material through the boundaries to within the precision limits of the CRAY I-S.

Results at the end of the simulation for the FTCS scheme are shown in Figure 34. Since the cell Peclet number limit of 2 is violated in the vicinity of the front, oscillations develop behind the movement of the front. Mass is conserved in the simulation, at the expense of negative concentrations and cell concentrations greater than 10.0.

The three FCT limiters developed previously [2] were tested. The original Zalesak limiter results are shown in Figure 35. Cell concentrations greater than 10.0 were developed. The alternative one (mixed time level) limiter results are shown in Figure 36. No cell concentrations exceed 10.0. However, the maximum allowable mass to enter a cell, Q^+, or leave, Q^- may now be negative unlike in the original limiter. Some small negative concentrations are also developed. The second alternative (previous time level) limiter results are shown in Figure 37. No cell concentrations exceed 10.0, Q^+ and Q^- are nonnegative, and no negative concentrations are developed.

Although all these versions of the limiter preserve mass, the second alternative (previous time level) limiter, based upon the nonnegativity of Q^+ and Q^-, appears to have some advantages over the other two limiters. Additional prototype simulations must be performed, however, before the final version of the limiter may be determined.

	N							
M	100	101	102	103	104	105	106	107
50	0.	0.	0.	0.	0.	0.	0.	0.
51	0.	0.	0.	0.	0.	0.	0.	0.
52	0.	0.	0.	0.	0.	0.	0.	0.
53	0.	20.	20.	20.	20.	21.	0.	0.
54	7.	9998.	9998.	9997.	9997.	9988.	0.	0.
55	12.	9961.	9960.	9959.	9959.	9944.	0.	0.
56	0.	0.	0.	0.	0.	0.	0.	0.
57	0.	0.	0.	0.	0.	0.	0.	0.

Figure 33. FTUS simulation global grid results at 5τ ($\times 10^3$)

	N							
M	100	101	102	103	104	105	106	107
50	0.	0.	0.	0.	0.	0.	-0.	0.
51	0.	0.	0.	0.	0.	0.	-0.	0.
52	0.	0.	0.	0.	0.	0.	-0.	0.
53	0.	10.	10.	10.	10.	10.	-0.	0.
54	4.	10009.	10005.	10005.	10005.	10001.	-4.	0.
55	6.	9985.	9979.	9978.	9978.	9970.	-6.	0.
56	0.	-14.	-14.	-15.	-15.	-16.	0.	-0.
57	0.	0.	0.	0.	0.	0.	-0.	0.

Figure 34. FTCS simulation global grid results at 5τ ($\times 10^3$)

	N							
M	100	101	102	103	104	105	106	107
50	0.	0.	0.	0.	0.	0.	0.	0.
51	0.	0.	0.	0.	0.	0.	0.	0.
52	0.	0.	0.	0.	0.	0.	0.	0.
53	0.	17.	16.	16.	16.	10.	0.	0.
54	6.	10001.	10001.	10001.	10001.	9996.	0.	0.
55	6.	9967.	9960.	9959.	9959.	9944.	0.	0.
56	0.	0.	0.	0.	0.	0.	0.	-0.
57	0.	0.	0.	0.	0.	0.	0.	0.

Figure 35. Original Zalesak FCT limiter global grid simulation results at 5τ ($\times 10^3$)

	N							
M	100	101	102	103	104	105	106	107
50	0.	0.	0.	0.	0.	0.	0.	0.
51	0.	0.	0.	0.	0.	0.	-0.	0.
52	0.	0.	0.	0.	0.	0.	-0.	0.
53	0.	18.	17.	17.	17.	11.	0.	0.
54	7.	10000.	10000.	10000.	10000.	9995.	0.	0.
55	6.	9967.	9960.	9959.	9959.	9944.	0.	0.
56	0.	0.	0.	0.	0.	0.	0.	0.
57	0.	0.	0.	0.	0.	0.	-0.	0.

Figure 36. Alternative one (mixed time level) FCT limiter global grid simulation results at 5τ ($\times 10^3$)

	N							
M	100	101	102	103	104	105	106	107
50	0.	0.	0.	0.	0.	0.	0.	0.
51	0.	0.	0.	0.	0.	0.	0.	0.
52	0.	0.	0.	0.	0.	0.	0.	0.
53	0.	20.	20.	20.	20.	17.	0.	0.
54	7.	9998.	9998.	9998.	9997.	9990.	0.	0.
55	7.	9966.	9960.	9959.	9959.	9944.	0.	0.
56	0.	0.	0.	0.	0.	0.	0.	0.
57	0.	0.	0.	0.	0.	0.	0.	0.

Figure 37. Alternative two (previous time level) FCT limiter global grid simulation results at 5τ ($\times 10^3$)

REFERENCES

1. Schmalz, R. A. The Development of a Numerical Solution to the Transport Equation; Report 1: Methodology, Miscellaneous Paper CERC-83-2, U. S. Army Engineer Waterways Experiment Station, Vicksburg, Miss., Sep 1983.

2. _____. The Development of a Numerical Solution to the Transport Equation; Report 2: Computational Procedures, Miscellaneous Paper CERC-83-2, U. S. Army Engineer Waterways Experiment Station, Vicksburg, Miss., Sep 1983.

3. Polzhiy, G. N. Equations of Mathematical Physics, New York: Hayden Book Co., Inc., 1967.

END

FILMED

11-83

DTIC